

LETTER TO THE EDITOR

## CO(4–3) and CO(7–6) maps of the nucleus of NGC 253

R. Güsten, S. D. Philipp, A. Weiß, and B. Klein

Max-Planck-Institut für Radioastronomie, Auf dem Hügel 69, 53121 Bonn, Germany  
e-mail: rguesten@mpi-fr-bonn.mpg.de

Received 18 April 2006 / Accepted 9 May 2006

### ABSTRACT

**Context.** Molecular line excitation studies of the nuclei of nearby starburst galaxies yield important information on the starburst phenomena, in particular on the temperature and density of the star-forming gas. Such studies also provide templates for high redshift galaxies with even more extreme star formation.

**Aims.** Fundamental constraints on the physical properties in the nuclear regions of external galaxies can be derived from the spectral energy distribution (i.e., integrated flux density vs. rotational quantum number) of CO rotational emission arising from warm gas.

**Methods.** The resolution and sensitivity of the APEX telescope makes it feasible to perform spatially resolved studies of submillimeter (submm) CO emission from the warm, dense gas in nearby starburst nuclei. Using the FLASH dual-channel heterodyne receiver we mapped emission in the CO  $J = 4-3$  and  $7-6$  lines toward the archetypical nuclear starburst galaxy NGC 253.

**Results.** Combining our new observations with data from the literature, we derive the CO line SED in the central 250 pc of NGC 253, which peaks near the  $6-5$  transition and has a shape very similar to that of M 82. All CO transitions in the central region can well be fitted with a single temperature/density Large Velocity Gradient (LVG) model. A good match to the observations is found by assuming kinetic gas temperatures that are comparable to the dust temperature ( $T_{\text{kin}} \approx 60$  K) and a  $\text{H}_2$  density of order  $10^4 \text{ cm}^{-3}$ .

**Conclusions.** Our very first APEX submm study of a nearby starburst nucleus (NGC 253) meaningfully constrains the physical properties of the star-forming molecular gas it contains. With broader band spectrometers and a chopping secondary coming soon, the impact of APEX on extragalactic astrophysics will be foreseeably significant.

**Key words.** ISM: molecules – galaxies: nuclei – galaxies: starburst

### 1. Introduction

In the warm, dense interstellar medium the mid-rotational transitions of carbon monoxide (rotational quantum number,  $J_{\text{up}}$ , from 4 to 8) are predicted to be the main cooling lines of the dense molecular gas. Therefore, studies of these lines will help to constrain its physical properties. In recent years, CO excitation studies have been extended to ultra-luminous objects with redshifts  $z > 2$ , for which these transitions are shifted to millimeter wavelengths (see e.g. Weiß et al. 2005a). Though faint, these lines are accessible then to classical millimeter observatories with their large collecting areas, operating with near quantum-limited detectors. In contrast, because observations from ground-based facilities of submm CO lines close to their rest frequencies are limited by Earth's poor atmospheric transmission, reference data on the "CO line SEDs" of nearby starburst nuclei are still scarce.

The Atacama Pathfinder EXperiment<sup>1</sup> opens new perspectives: the superb atmospheric transmission on Llano de Chajnantor will allow routine observations up to 900 GHz (including the  $J = 4-3$ ,  $J = 6-5$ , and  $J = 7-6$  transitions), with the possibility of dedicated experiments even in the supra-THz windows (e.g., CO(9–8) at 1037 and CO(14–13) at 1497 GHz).

The first extragalactic object at which the APEX was pointed during its commissioning was NGC 253, which is considered, together with M 82 the archetypical nuclear starburst galaxy.

Due to its relative proximity ( $D = 3.5$  Mpc, Rekola et al. 2005,  $1''$  corresponds to 17 pc), the circumnuclear gas layer (extending  $\sim 40'' \times 15''$  ( $680 \times 250$  pc) at position angle  $58^\circ$ , e.g. Sakamoto et al. 2006) is resolved with APEX (our  $7.7''$  FWHM beam at 806 GHz corresponds to 131 pc). The starburst proper, which took place 5.5 (Tacconi-Garman 2006) to 20 Myr (Engelbracht et al. 1998) ago, is confined to the central  $5''-10''$ , releasing a far-infrared luminosity  $\sim 10^{10.5} L_\odot$  (Rice et al. 1988). The molecular gas is known to be dense and warm (Israel et al. 1995; Bayet et al. 2004), although the details of its excitation are discussed controversial.

NGC 253 is the brightest extragalactic (line) source on the submm sky, but – due to its low elevation – surprisingly few observations have been targeted at its prominent nucleus. After the first detections of warm CO(4–3) (Güsten et al. 1993) and CO(6–5) (Harris et al. 1991), only recently Bayet et al. (2004) mapped the central layer in CO(6–5). Bradford et al. (2003) present a single exposure with their Fabry-Perot interferometer array, scanning the CO(7–6) emission.

In this paper we present CO(4–3) and CO(7–6) maps of the central nuclear disk obtained with APEX. Different to northern observatories, the source can be observed at low air masses with superb atmospheric transmission, thus providing – potentially – better calibrated data.

### 2. Observations

The observations were performed in June ( $J = 4-3$ , 461.04 GHz) and October 2005 ( $J = 7-6$ , 806.65 GHz), using the MPIFR Principal Investigator instrument FLASH

<sup>1</sup> This publication is based on data acquired with the Atacama Pathfinder EXperiment. APEX is a collaboration between the Max-Planck-Institut für Radioastronomie, the European Southern Observatory, and the Onsala Space Observatory.

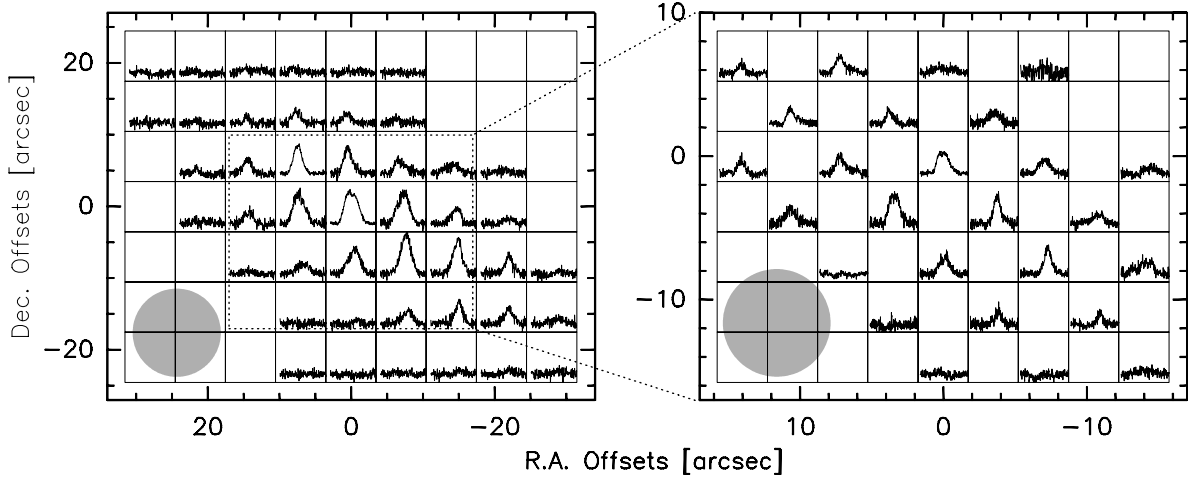


**Fig. 1.** CO(4–3) and CO(7–6) spectra maps toward the nucleus of NGC 253 (RA = 00<sup>h</sup>47<sup>m</sup>32<sup>s</sup>.98; Dec = –25°17′15.9″, J2000). Spectra are shown on a velocity scale from –110 to 550 km s<sup>–1</sup> and on a  $T_{\text{mb}}$  brightness temperature scale ranging from –1.5 to 7.5 K for both data sets. Spectra have been observed on a regular raster with spacings of 7″ (the  $J = 7–6$  data with an interleaved 3.5″ grid). The half power beam widths of the observations are shown for reference (13.3″ and 7.7″, resp.).

**Table 1.** Line parameters at different angular resolutions toward the central position in NGC 253.

| Transition | beam<br>[″]       | $\int T_{\text{mb}} dv$<br>[K km s <sup>–1</sup> ] | $\int S_{\nu} dv$<br>[Jy km s <sup>–1</sup> ] | Flux<br>[W m <sup>–2</sup> ] |
|------------|-------------------|--|---|------------------------------|
| CO(4–3)    | 13.3 <sup>a</sup> | 1240   | 38 150  | $5.9 \times 10^{-16}$        |
| CO(7–6)    | 7.7 <sup>a</sup>  | 830  | 26 200  | $7.0 \times 10^{-16}$        |
| CO(4–3)    | 15                | 1040   | 41 900  | $6.4 \times 10^{-16}$        |
| CO(7–6)    | 15                | 380  | 44 950  | $1.2 \times 10^{-15}$        |
| CO(4–3)    | 22                | 700  | 58 900  | $9.1 \times 10^{-16}$        |
| CO(7–6)    | 22                | 245  | 63 150  | $1.7 \times 10^{-15}$        |

Note: spectra have been numerically convolved to 15 and 22″ angular resolution. We assign uncertainties of 15 [CO(4–3)] and 20% [CO(7–6)], at original (<sup>a</sup>) and 15″ resolution. For the 22″ beam, the error is larger (20, 30%), because emission may extend beyond our map sizes.

(Heyminck et al. 2006) during stable night time conditions. Atmospheric transmissions were excellent (with 0.3 and 0.4 mm precipitable water only), yielding system temperatures as low as 500 (FLASH-I) and 1100 K (FLASH-II).

Pointing was established by total power continuum slews across Mars and by CO(4–3) line pointing on  $\alpha$  Ceti. For the observations of NGC 253, we frequently monitored the line profile of the nominal center position and corrected the pointing offsets if necessary. For these observations the pointing accuracy should therefore be better than 2–3″. Focus alignment was verified on Mars. The  $FWHM$  beam size of the telescope at the CO(4–3) and (7–6) frequencies is 13.3″ and 7.7″, respectively. CO(4–3) data were fully sampled on a regular raster with 7″ spacing in right ascension and declination, centered at (RA = 00<sup>h</sup>47<sup>m</sup>32<sup>s</sup>.98; Dec = –25°17′15.9″ (J2000)). CO(7–6) was measured beam-spaced (7″), with an interleaved grid (see Fig. 1). All spectra were observed in total power mode by switching every 20 s to a nearby reference position, offset by 60″ in RA.

Calibration was obtained with the APEX calibration software (Muders et al. 2006). All spectra presented here are in units of main-beam brightness temperature ( $T_{\text{mb}}$ ), corrected for atmospheric transmission in both sidebands and the proper telescope efficiencies. The forward-coupling and main-beam efficiencies for FLASH are (0.95, 0.60) and (0.95, 0.43),

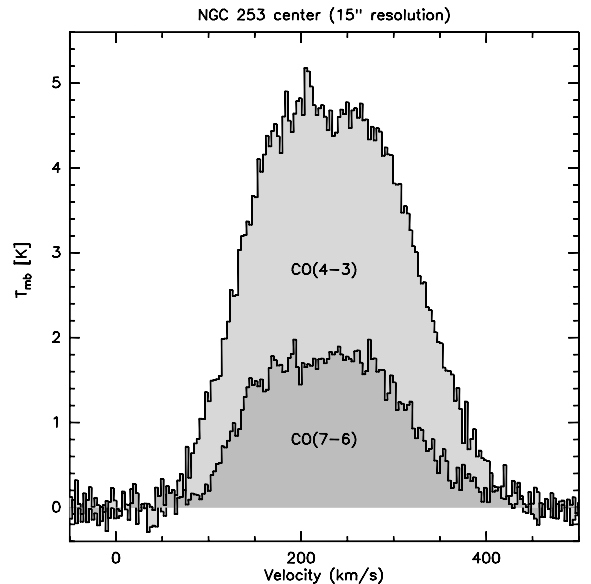


**Fig. 2.** CO(4–3) and CO(7–6) spectra, convolved to 15″ angular resolution, toward the center of NGC 253.

respectively (Güsten et al. 2006). The data were processed with the MPIfR FFT spectrometers (Klein et al. 2006) providing – at that time –  $2 \times 1$  GHz of bandwidth, with 16 384 channels each. The spectra were smoothed to appropriate resolutions. For the CO(7–6) 806 GHz measurements the two backends were stacked in series with 200 MHz of overlap, thus providing the necessary bandwidth (1.8 GHz = 670 km s<sup>–1</sup>) to study the broad-line emission from the NGC 253 nucleus. The intermediate frequency (IF) was centered on the systemic velocity of 240 km s<sup>–1</sup>. All further data processing was performed with the CLASS software. The data presented here have been re-gridded to 6 km s<sup>–1</sup> velocity resolution. Only linear baselines have been removed from the spectra.

### 3. Results

CO(4–3) spectra toward 45 positions nicely trace the warm circumnuclear disk. The more difficult to observe CO(7–6) lacks

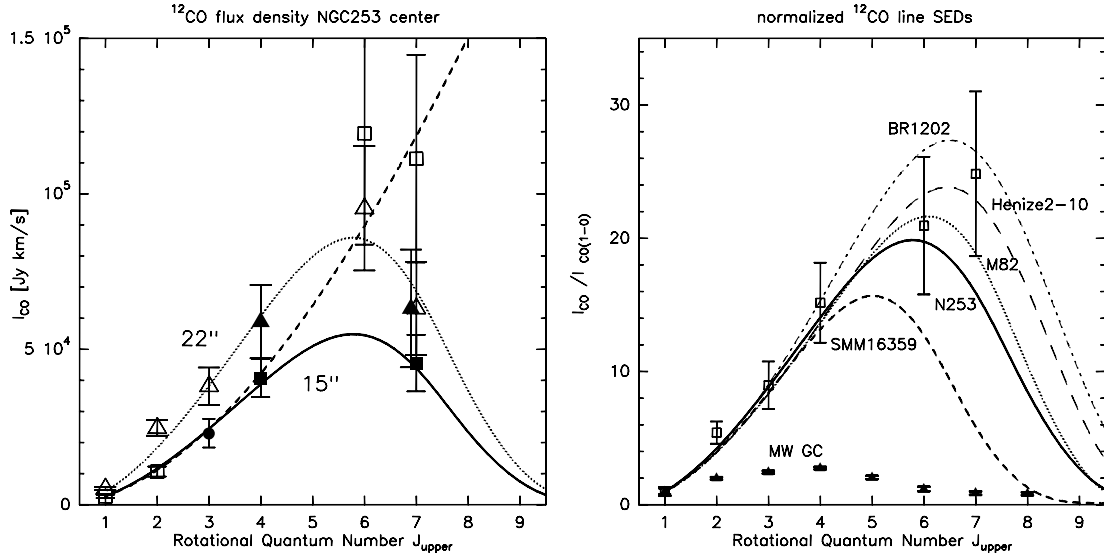


**Fig. 3.** *Left:* velocity-integrated CO flux densities vs. rotational quantum number (“CO line SED”). Squares indicate the integrated flux densities for  $15''$ , triangles for  $22''$  angular resolution. Filled symbols are from this paper (Table 1) and from Israel et al. (1995), open squares were adopted from Bradford et al. (2003), open triangle from Bayet et al. (2004). The lines show the LVG-predicted fluxes for  $n(\text{H}_2)$ ,  $T_{\text{kin}}$  and beam filling factors of  $10^{3.9} \text{ cm}^{-3}$ , 60 K, 11% ( $15''$  beam, solid),  $10^{3.9} \text{ cm}^{-3}$ , 60 K, 8% ( $22''$  beam, dotted) and optically thick, thermalized CO emission at 100 K with a filling factor of 5% ( $15''$  beam, dashed). *Right:* comparison of various normalized CO line SEDs: SEDs are shown for BR1202-0725 ( $z = 4.7$ , dashed-dotted curve, no data plotted, Carilli et al. 2002; Riechers et al. 2006), Henize2–10 (long-dashed curve, open squares, Bayet et al. 2004), the high-excitation component in the center of M 82 (dotted curve, no data plotted, Weiß et al. 2005b), NGC 253 center (same model as the solid line to the left), SMMJ16359+6612 (dashed curve, no data plotted, Weiß et al. 2005a) and the Galactic Center (filled triangles, Fixsen et al. 1999).

some emission toward the north-east. A fully sampled map in this line has to await our CHAMP<sup>+</sup> (Kasemann et al. 2006) array to become operational later this year. Both maps outline the elongated central molecular gas layer seen in lower CO transitions at similar resolution (see e.g. Israel et al. 1995; Mauersberger et al. 1996), and in particular with interferometric high angular resolution maps (e.g. Sakamoto et al. 2006). Peak main-beam temperatures ( $7.2$  and  $5.4 \text{ K}$  in CO(4–3) and (7–6), respectively) are strongest toward the super star cluster identified by Keto et al. (1999), offset from the radio nucleus and the kinematic center. The asymmetry along the disk seen in our data, with a more prominent south-western lobe, resembles the distribution reported for other star formation tracers like the emission of PAHs (Tacconi-Garman et al. 2005) and of  $\text{H}_2$  ( $v = 1-0$ ) (Sugai et al. 2003).

Eliminating differential beam-coupling effects to first order by convolving the spectra to identical beam size ( $15''$ , see below), reveals  $T_{\text{mb}}^{4-3}/T_{\text{mb}}^{7-6} \sim 2.7$  – a finding that is important for our later analysis of the turn-over in the CO line SED. The line luminosities integrated over our maps are  $2.6 \times 10^8$  and  $8.0 \times 10^7 \text{ K km s}^{-1} \text{ pc}^2$  for CO(4–3) and CO(7–6), respectively. Comparing our results with data published in the literature, we notice significant differences to brightnesses quoted for these submm lines. Our velocity-integrated temperature for the CO(4–3) line ( $1240 \text{ K km s}^{-1}$  within our  $13.3''$  beam, Table 1) are not consistent with temperatures quoted by Israel et al. (1995) ( $2150 \text{ K km s}^{-1}$  in their  $10.6''$  beam). However, our calibration does compare with more recent data from the JCMT<sup>2</sup>, yielding lower figures of  $1350 \text{ K km s}^{-1}$  and  $900 \text{ K km s}^{-1}$ . Our CO(7–6) integrated brightness ( $830 \text{ K km s}^{-1}$  in the  $7.7''$  beam, again Table 1) is lower than the intensity published by

Bradford et al. ( $1370 \text{ K km s}^{-1}$ ,  $11.5''$  beam), but compares with the result quoted in Bayet et al. ( $810 \text{ K km s}^{-1}$ ,  $9''$  beam). We notice, however, that – in comparison to our (0,0) spectrum – the profile shown in Bayet et al. is rather narrow with a higher peak line temperature, more resembling the profiles in our map with slight offset positions from the nominal center.

#### 4. Analysis

We combine our new CO(4–3) and CO(7–6) maps with data from the literature to re-visit the CO excitation toward the center of NGC 253. For this we smoothed our data cubes to  $15''$  and  $22''$  resolution (these are the resolutions used by Bradford et al. 2003; Bayet et al. 2004). In Fig. 2 we display the APEX spectra, convolved to  $15''$  resolution. Line intensities for different angular resolutions are given in Table 1. The spectral energy distribution of the CO lines (“CO line SED”) is shown in Fig. 3 (see the figure caption for references and details).

To investigate the CO excitation in more detail we used a spherical, one-component large velocity gradient (LVG) model. We use the collision rates from Flower (2001) with an ortho/para  $\text{H}_2$  ratio of 3 and a CO abundance per velocity gradient of  $[\text{CO}]/dv/dr = 10^{-5} \text{ pc (km s}^{-1})^{-1}$  (Weiß et al. 2005b). For both resolutions all lines are well fit with a single LVG model if we consider our data and the values given by Bayet et al. For the data at  $15''$  resolution a good fit to the observations is provided by  $n(\text{H}_2) = 10^{3.9} \text{ cm}^{-3}$ , a temperature of  $T_{\text{kin}} = 60 \text{ K}$  (not too far from the central dust temperature of  $50 \text{ K}$ , Melo et al. 2002), and a beam filling factor of 11%. The same model also matches the data at  $22''$  resolution if the filling factor is scaled to 8%. These models are shown superimposed on the observations in Fig. 3 (left). For a fractional  $^{13}\text{CO}$  abundance of  $X[^{12}\text{CO}]/X[^{13}\text{CO}] = 60$  this model also reproduces the observed  $^{13}\text{CO}$  intensities. Other temperature-density combinations with similar  $\text{H}_2$  pressure do also fit the data, in particular if we allow

<sup>2</sup> We are very grateful to Frank Israel who made available these unpublished JCMT observations, obtained in late 1994 and 1998, thus creating independent confidence in the APEX calibration scheme.

for variations of the CO abundance per velocity gradient and the fractional  $^{13}\text{C}$  abundance (see e.g. Bradford et al. 2003). From Fig. 3 it is clear, that the CO line SED for the center of NGC 253 peaks near the CO(6–5) line. Comparing the predicted CO(2–1) Planck-temperature of 55 K with the minimum Planck temperature of 41 K derived by Sakamoto et al. from their interferometric data, we confirm their conclusion about the high filling factor of the gas in their  $4.3'' \times 2.5''$  beam.

## 5. Discussion

Our measurements and derived gas parameters are different from those obtained by Bradford et al. (2003). As shown in Fig. 3 (left) these differences mainly arise from our lower CO(7–6) line intensity toward the nucleus of NGC 253. Based on the CO(1–0) to CO(4–3) intensities at  $15''$  resolution, it is, however, very unlikely that the CO(7–6) line could be as bright as measured by Bradford et al. For this the CO emission would have to be thermally excited up to CO(7–6) in the optically thick limit (see the dashed curve in Fig. 3 left). This would imply that the CO flux density of transitions with  $J_{\text{up}} > 7$  would still increase dramatically. Such a CO SED would also be different from what has been found in other starburst galaxies in the local universe (such as M 82) and in much more (IR) luminous galaxies at high redshift. This is visualized in Fig. 3 (right) where we compare the CO line SEDs of nearby and high- $z$  galaxies to those derived here in NGC 253. The fits to our CO data as well as to those by Bayet et al. (2005) yield a CO line SED very similar to that in the center of M 82 (e.g. Weiß et al. 2005b), where the peak of the CO SED also occurs at the CO(6–5) line. Higher CO excitation with a peak around the CO(7–6) line is seen toward some high- $z$  QSO host galaxies such as BR 1202-0751 (Carilli et al. 2002; Riechers et al. 2006) and in the blue compact dwarf galaxy Henize2–10 (Bayet et al. 2004) while the peak for high- $z$  pure starburst galaxy SMM 16359+6612 ( $z = 2.5$ ) already occurs at the CO(5–4) line (Weiß et al. 2005a). Local systems

with lower nuclear activity seem to have lower CO excitation as visualized by the CO SEDs from the Galactic Centre.

Our very first submm study with APEX of a nearby starburst nucleus reveals the potential of the facility in constraining the gas excitation in these nuclei. It also demonstrates, however, the difficulties in obtaining precise enough flux measurements at submm wavelengths. With broader band spectrometers and a chopping secondary coming soon, and given the exceptionally good atmospheric transmission from Llano de Chajnantor, the impact of APEX on extragalactic astronomy will foreseeably be significant.

## References

- Bayet, E., Gerin, M., Phillips, T. G., et al. 2004, *A&A*, 427, 45  
Bradford, C. M., Nikola, T., Stacey, G. J., et al. 2003, *ApJ*, 586, 891  
Carilli, C. L., Kohno, K., Kawabe, R., et al. 2002, *AJ*, 123, 1838  
Engelbracht, C. W., Rieke, M. J., Rieke, G. H., et al. 1998, *ApJ*, 505, 639  
Fixsen, D. J., Bennett, C. L., & Mather, J. 1999, *ApJ*, 526, 207  
Flower, D. R. 2001, *J. Phys. B: At. Mol. Phys.*, 34, 2731  
Güsten, R., Nyman, L.-Å., Schilke, P., et al. 2006, *A&A*, 454, L13  
Güsten, R., Serabyn, E., Kasemann, C., et al. 1993, *ApJ*, 402, 537  
Harris, A. I., Stutzki, J., Graf, U. U., et al. 1991, *ApJ*, 382, L75  
Heyminck, S., Kasemann, C., Güsten, R., et al. 2006, *A&A*, 454, L21  
Israel, F. P., White, G. J., & Baas, F. 1995, *A&A*, 302, 343  
Kasemann, C., Güsten, R., Heyminck, S., et al. 2006, in *Proc. SPIE*, 6275, in preparation  
Keto, E., Hora, J. L., Fazio, G. G., et al. 1999, *ApJ*, 518, 183  
Klein, B., Philipp, S. D., Krämer, I., et al. 2006, *A&A*, 45, L29  
Mauersberger, R., Henkel, C., Wielebinski, R., et al. 1996, *A&A*, 305, 421  
Melo, V. P., Pérez García, A. M., Acosta-Pulido, J. A., Muñoz-Tuñón, C., & Rodríguez Espinosa, J. M. 2002, *ApJ*, 574, 709  
Muders, D., Hafok, H., Wyrowski, F., et al. 2006, *A&A*, 454, L25  
Rekola, R., Richer, M. G., McCall, M. L., et al. 2005, *MNRAS*, 361, 330  
Rice, W., Lonsdale, C. J., Soifer, B., et al. 1988, *ApJS*, 68, 91  
Riechers, D. A., Weiß, A., Walter, F., et al. 2006, *ApJ*, in press  
Sakamoto, K., Ho, P. T. P., Iono, D., et al. 2006, *ApJ*, 636, 685  
Sugai, H., Davies, R. I., & Ward, M. J. 2003, *ApJ*, 584, L9  
Tacconi-Garman, L. E. 2006, *New Astron. Rev.*, 49, 569  
Tacconi-Garman, L. E., Sturm, E., Lehnert, M., et al. 2005, *A&A*, 432, 91  
Weiß, A., Downes, D., Walter, F., et al. 2005a, *A&A*, 440, L45  
Weiß, A., Walter, F., & Scoville, N. Z. 2005b, *A&A*, 438, 533